

## LETTER TO THE EDITOR

### Photoionization of Fe<sup>+</sup>

Maryvonne Le Dourneuff, Sultana N Nahar‡ and Anil K Pradhan‡

† Laboratoire de Théorie des Processus Atomiques et Moléculaires, UPR 261 du CNRS, Observatoire de Paris, 92195 Meudon, France

‡ Department of Astronomy, The Ohio State University, Columbus, OH 43210, USA

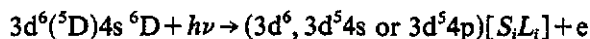
Received 10 November 1992

**Abstract.** New results are presented for the photoionization of Fe<sup>+</sup> in the close-coupling approximation using the *R*-matrix method. Cross sections are reported for the <sup>6</sup>D symmetry, including the ground state 3d<sup>6</sup>4s(<sup>6</sup>D). The effect of photoionization of the 4s and the 3d shells is investigated through a series of calculations and it is shown that the latter makes the dominant contribution. The final 21-state expansion for the core ion Fe<sup>2+</sup> includes all coupled states from the 3d<sup>6</sup>, 3d<sup>5</sup>4s and 3d<sup>5</sup>4p configurations. Photoionization of bound states along a Rydberg series is studied and the influence of strong photoexcitation-of-core type of resonances is pointed out. Partial cross sections for photoionization into individual final states of the core ion are also obtained. The new ground state cross section is up to two orders of magnitude higher than recently reported values.

Although Fe<sup>+</sup> is an ion of enormous importance in astrophysics, its complex electronic structure with a large number of closely spaced energy levels makes it difficult to carry out *ab initio* atomic calculations and the little previous work that has been reported is not accurate. The primary effect to take into account is the strong coupling between the various photoionization channels belonging to a number of excited states of the residual ion and orbital angular momenta of the continuum electron. The close-coupling method enables a detailed consideration of the coupling and related effects due to autoionization structures. However, the first step in the close-coupling calculations, that is to determine an adequately large and accurate wavefunction expansion for the states of the residual or the 'target' ion, involves extensive atomic structure calculations. Furthermore, the convergence of the expansion as it relates to the contribution to the total photoionization cross section from the excited states is not apparent from the term energy diagram. In particular, the relative contributions from the 4s and 3d outer shells need to be studied as one expects that the open 3d shell will play an important role in the photoionization of the ground state and other low lying states.

The factors outlined above require that several sets of calculations, with successively more extensive eigenfunction expansions, are needed to properly study the effect of convergence and resonances. In the present report we focus on the <sup>6</sup>D states, particularly the ground state 3d<sup>6</sup>(<sup>5</sup>D)4s <sup>6</sup>D and discuss some of the calculations that have been carried out using the *R*-matrix method. The computer codes employed were developed for the Opacity Project (Seaton 1987) and are described by Berrington *et al* (1987).

We consider the ground state photoionization of Fe<sup>+</sup>,



where the right-hand side represents the final states  $S_i L_i$  of the residual ion  $\text{Fe}^{2+}$  dominated by any one of the three configurations listed, which altogether give rise to 136  $LS$  terms of septet, quintet, triplet and singlet symmetries. Thus for the photoionization of  $\text{Fe}^+$  the total symmetries for the (electron+ion) system to be considered are: octets, sextets, quartets and doublets.

As we confine ourselves to  ${}^6D$  states of  $\text{Fe}^+$ , only the septet and the quintet states of  $\text{Fe}^{2+}$  are coupled in the calculations. The target ion expansion for  $\text{Fe}^{2+}$  was developed using the SUPERSTRUCTURE program of Eissner *et al* (1974). The configuration basis, with the three primary configurations and five correlation configurations, is given in table 1. It was chosen to optimize primarily the 3d shell correlation. The 21 states of  $\text{Fe}^{2+}$  so obtained are also listed in table 1 along with their experimental and calculated energies.

Table 1. Energies (in Rydbergs) of the 21 target terms of  $\text{Fe}^{2+}$ . Note: the experimental energies are from Sugar and Corliss (1985). The  $\text{Fe}^{2+}$  eigenfunction expansion consists of the following: primary configurations:  $3s^2 3p^6 3d^6$ ,  $3s^2 3p^6 3d^5 4s$ ,  $3s^2 3p^6 3d^5 4p$ ; correlation configurations:  $3s^2 3p^4 3d^8$ ,  $3p^6 3d^8$ ,  $3s 3p^6 3d^7$ ,  $3s 3p^5 3d^8$ ,  $3s^2 3p^6 3d^5 4d$ .

| Term                             | $E$ (expt) | $E$ (calc.) | Term                             | $E$ (expt) | $E$ (calc.) |
|----------------------------------|------------|-------------|----------------------------------|------------|-------------|
| 1 $3d^6$ ${}^5D$                 | 0.0000     | 0.0000      | 12 $3d^5({}^4G)4p$ ${}^5F^\circ$ | 1.0619     | 1.0717      |
| 2 $3d^5({}^6S)4s$ ${}^7S$        | 0.2742     | 0.2729      | 13 $3d^5({}^4P)4p$ ${}^5D^\circ$ | 1.0661     | 1.0825      |
| 3 $3d^5({}^6S)4s$ ${}^5S$        | 0.3736     | 0.4167      | 14 $3d^5({}^4P)4p$ ${}^5S^\circ$ | 1.0653     | 1.0847      |
| 4 $3d^5({}^4G)4s$ ${}^5G$        | 0.5783     | 0.5995      | 15 $3d^5({}^4P)4p$ ${}^5P^\circ$ | 1.0810     | 1.1083      |
| 5 $3d^5({}^4P)4s$ ${}^5P$        | 0.6061     | 0.6466      | 16 $3d^5({}^4P)4p$ ${}^5F^\circ$ | 1.1041     | 1.1220      |
| 6 $3d^5({}^4D)4s$ ${}^5D$        | 0.6359     | 0.6730      | 17 $3d^5({}^4P)4p$ ${}^5D^\circ$ | 1.1208     | 1.1449      |
| 7 $3d^5({}^6S)4p$ ${}^7P^\circ$  | 0.7516     | 0.7338      | 18 $3d^5({}^4D)4p$ ${}^5P^\circ$ | 1.1272     | 1.1509      |
| 8 $3d^5({}^4F)4s$ ${}^5F$        | 0.7585     | 0.8038      | 19 $3d^5({}^4F)4p$ ${}^5G^\circ$ | 1.2339     | 1.2602      |
| 9 $3d^5({}^6S)4p$ ${}^5P^\circ$  | 0.8133     | 0.8295      | 20 $3d^5({}^4F)4p$ ${}^5F^\circ$ | 1.2402     | 1.2716      |
| 10 $3d^5({}^4G)4p$ ${}^5G^\circ$ | 1.0358     | 1.0353      | 21 $3d^5({}^4F)4p$ ${}^5D^\circ$ | 1.2520     | 1.2848      |
| 11 $3d^5({}^4G)4p$ ${}^5H^\circ$ | 1.0512     | 1.0507      |                                  |            |             |

In addition to the energies listed in table 1, a careful examination was made of the agreement between the length and the velocity oscillator strengths for transitions among the  $3d^6$ ,  $3d^5 4s$  states of even parity and the  $3d^5 4p$  states of odd parity. The level of such an agreement is usually a good indicator of the accuracy of the target wavefunctions. We find that for most of over 300 transitions the agreement between length and velocity was around 15%. While this is somewhat larger than the usual aim of within 10%, given the complexity of the atomic structure calculations we consider this to be sufficient, as any further improvement would require a significantly larger basis set of correlation functions that might make the whole calculation impractical.

In order to study the effect of coupling of the final ion states on the photoionization cross sections, several sets of calculations were carried out using 3, 6, 9 and 21 states, respectively, of  $\text{Fe}^{2+}$ . Henceforth we refer to these as the 3CC, 6CC etc. The 3CC calculation included only the first three states,  $3d^6$   ${}^5D$  and  $3d^5({}^6S)4s$   ${}^7S$  and  ${}^5S$ , the 6CC included the next three additional states, the 9CC included the first nine states that contain two odd parity  $3d^5 4p$  states, and finally the 21CC calculation included all of the septet and the quintet states of table 1.

The final continuum state wavefunctions for the  ${}^6P^\circ$ ,  ${}^6D^\circ$  and the  ${}^6F^\circ$  symmetries were obtained at a fine mesh of the photoelectron energies, chosen to delineate the

resonance structures in detail. The mesh was chosen to be in terms of the effective quantum number,  $\nu$ , relative to successive target thresholds, such that an interval in  $\nu$  of 1.0 is delineated by 100 points; often this corresponds to the same number of points for an energy region containing one or two resonances. All resonances with  $\nu \leq 10.0$  are delineated fully.

Figure 1 presents the total cross sections for the ground state. As more states of the residual ion  $\text{Fe}^{2+}$  are included, the open channel region fills up with resonance structures belonging to the higher thresholds. In each figure, the last of the resonance structures corresponds to the highest threshold, as shown by arrows, in that particular approximation. For example, the 3CC results in figure 1(a) include the  $3d^6\ ^5D$ ,  $3d^5(^6S)4s\ ^7S$  and  $3d^5(^6S)4s\ ^5S$  states, and thus there are no resonances above the highest  $^5S$  state. In figure 1 the first arrow corresponds to the ionization threshold in that particular approximation.

A very large increment in the cross section is obtained over the 3CC results when a few other  $3d^54s$  states are included, as may be seen from figure 1(b) with the 6CC values. The *background* cross section increases by approximately a factor of two due to the coupling of the additional states. This points to the importance of the 3d shell in the photoionization process; the 6CC calculations include most of the contribution to ground state photoionization from the 4s and the 3d shells. The 9CC calculations in figure 1(c), with a few of the odd parity states dominated by the  $3d^54p$  configuration, contain more resonances but no significant increase in the background cross section over the 6CC results. The 21CC results show yet more resonance structure but these are rather weak, reflecting the weakening effect of coupling to higher states.

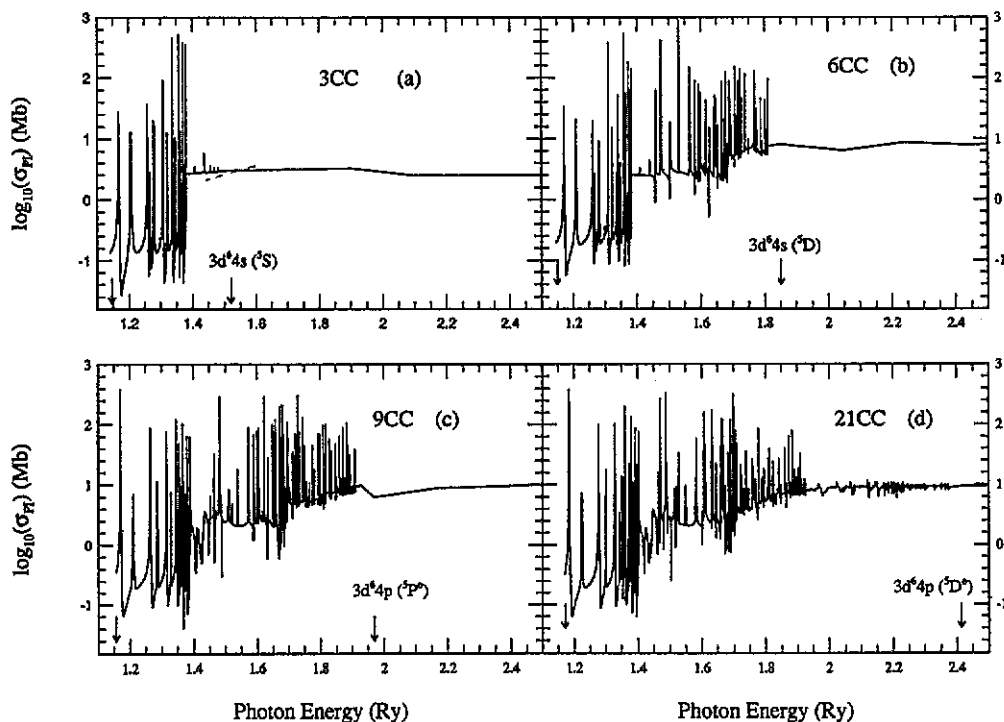


Figure 1. Ground state photoionization in the three-state, six-state, nine-state and 21-state close-coupling approximation.

The final 21CC cross sections for the ground state of  $\text{Fe}^+$  are up to two orders of magnitude higher than the recently reported values by Sawey and Berrington (1992) who employed only a single state expansion for  $\text{Fe}^{2+}$  and obtained a nearly constant value of 0.1 Mb, compared to the present maximum value of approximately 10 Mb for the background cross section (figure 1(d)). The cross sections reported by Reilman and Manson (1979) in the central field approximation (which does not account for coupling or resonance effects) are more than a factor of two lower in the near-threshold region than the present values.

Figure 2 shows the partial cross sections for photoionization of the ground state of  $\text{Fe}^+$  into several states of  $\text{Fe}^{2+}$ . As the incident photon energy increases to enable higher thresholds of the residual ion to be attained, the photoelectron flux redistributes itself into all the open channels at each threshold and one may calculate the partial photoionization cross sections for ionization into specific excited states of the residual ion (e.g. Nahar and Pradhan 1991). Under conditions of photoionization equilibrium and non-LTE stellar atmospheres the level population in excited states of ions is often determined by such partial photoionization from the previous ionization stage and it is useful to compute these cross sections explicitly. The arrow in each panel of figure 2 corresponds to the excited threshold of the residual ion. While we have calculated

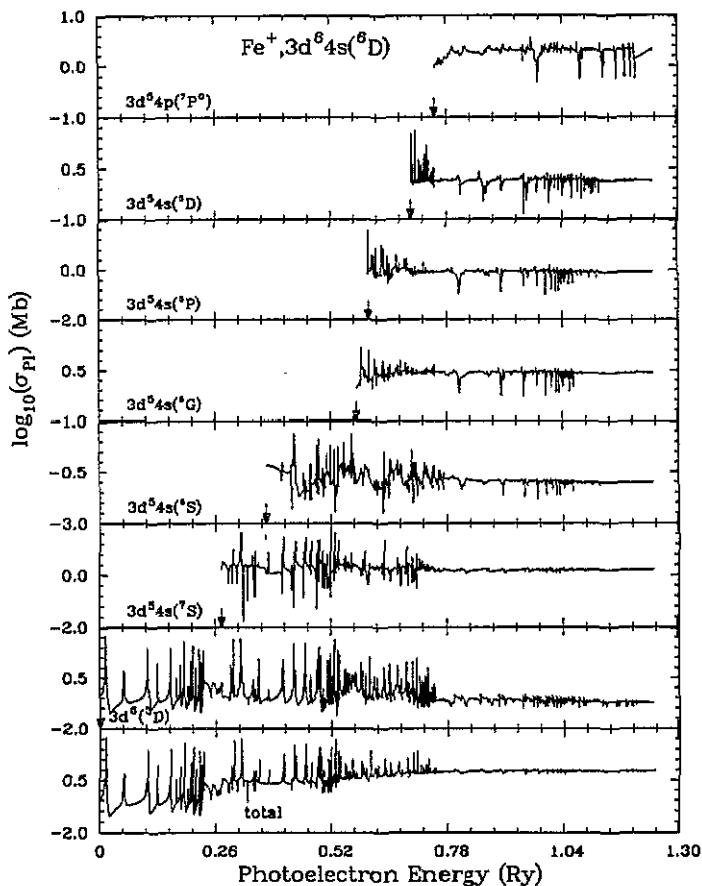
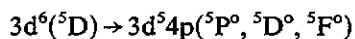


Figure 2. Cross sections for partial photoionization of the  $\text{Fe}^+$  ground state into the ground and the excited states of the residual ion  $\text{Fe}^{2+}$ .

the partial cross sections for ionization into all coupled states included in the  $\text{Fe}^{2+}$  expansion, the results are given only for a few selected states in the figure.

Yu and Seaton (1987) have described strong resonance features in the photoionization of excited Rydberg states associated with dipole allowed transitions *within* the residual ion core, and have labelled these as *photoexcitation-of-core* (PEC) resonances. The PEC resonances are related to the dielectronic recombination process in that the free electron may recombine with the ion through these resonances if they undergo radiative stabilization by emitting a photon—the inverse process. For photoionization of bound states of  $\text{Fe}^+$  in the Rydberg series  $3d^6(^5D)nd$ , for example, the PEC features correspond to dipole transitions of the type



in the  $\text{Fe}^{2+}$  core. As the outer electron is essentially a 'spectator' during the process, the PEC features are most easily discernible in the photoionization of bound states along a Rydberg series with weakly bound electrons. In these cases the PEC resonances modify considerably what one would otherwise expect to be a hydrogenic cross section.

Figure 3 shows the photoionization cross sections of bound states of the  $3d^6(^5D)nd\ ^6D$  series of  $\text{Fe}^+$ . The PEC resonances are the broad features lying in between

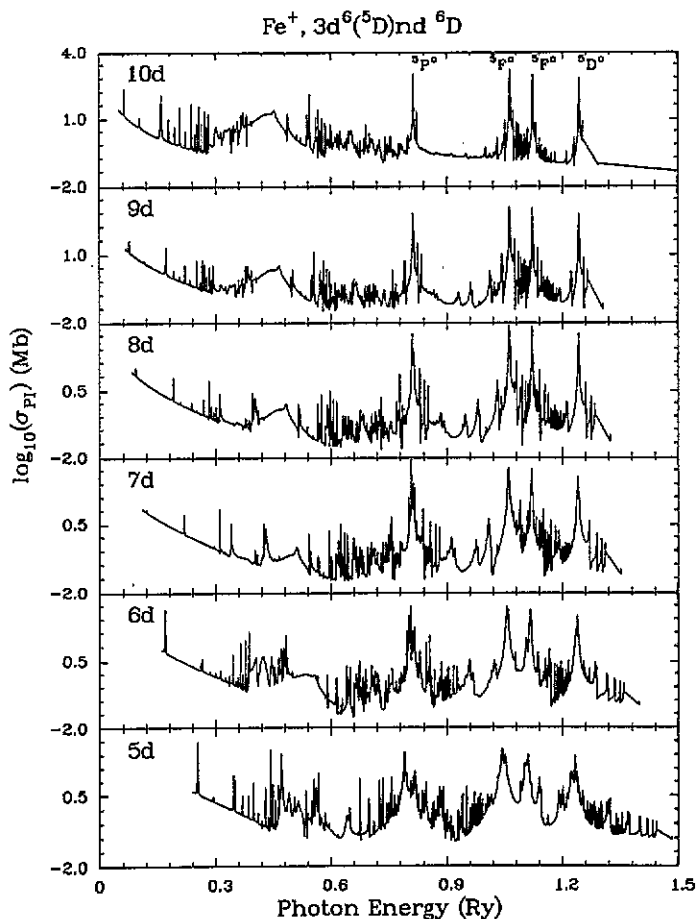


Figure 3. Photoionization cross sections of bound states of  $\text{Fe}^+$  in a Rydberg series showing the PEC resonance features.

the usual, narrower series of resonances converging onto the excited thresholds. As seen on looking up the panels of figure 3, the cross sections for all states along the Rydberg series of bound states show that the PEC resonances are at precisely the same photon energies corresponding to the dipole transitions within the  $\text{Fe}^{2+}$  core states. The prominent PEC resonances are identified in the figure.

Further calculations are in progress for the Opacity Project for photoionization cross sections and transition probabilities involving a large number of bound states of  $\text{Fe}^+$ , including the quartet and the doublet symmetries and up to 83 target terms in the  $\text{Fe}^{2+}$  eigenfunction expansion (perhaps the largest close-coupling calculations to date).

MLD would like to acknowledge support of the CNRS, France. This work was supported in part by grants from the US National Science Foundation (AST-8996215 and PHY-9115057). SNN acknowledges support from the College of Mathematical and Physical Sciences at the Ohio State University. The computational work was carried out at the Centre de Calcul Vectoriel pour la Recherche at Palaiseau (France) under grant 1607, and the Ohio Supercomputer Center in Columbus, Ohio (USA).

## References

- Berrington K A, Burke P G, Butler K, Seaton M J, Storey P J, Taylor K T and Yu Yan 1987 *J. Phys. B: At. Mol. Phys.* **20** 6379
- Eissner W, Jones M and Nussbaumer H 1974 *Comput. Phys. Commun.* **8** 270
- Nahar S N and Pradhan A K 1991 *Phys. Rev. A* **44** 2935
- Reilman R F and Manson S T 1979 *Astrophys. J. Suppl.* **40** 815
- Sawey P M J and Berrington K A 1992 *J. Phys. B: At. Mol. Opt. Phys.* **25** 1451
- Seaton M J 1987 *J. Phys. B: At. Mol. Phys.* **20** 6363
- Sugar J and Corliss C 1985 *J. Phys. Chem. Ref. Data* **14** Suppl. 2
- Yu Yan and Seaton M J 1987 *J. Phys. B: At. Mol. Phys.* **20** 6409